

## Experimental VNIR reflectance spectroscopy of gypsum dehydration: Investigating the gypsum to bassanite transition

TANYA N. HARRISON\*

Department of Earth and Environmental Sciences, Wesleyan University, 265 Church Street, Middletown, Connecticut 06459, U.S.A.

### ABSTRACT

The spectral behavior of gypsum dehydration in the visible to near-infrared (350–2500 nm) wavelength range was investigated by partially dehydrating the four main habits of gypsum (alabaster, satin spar, selenite, and massive) to form bassanite. Powdered samples of gypsum dehydrated at 100–115 °C and hand samples dehydrated at 115–130 °C, coinciding with a peak in mass (water) loss in the samples. As gypsum dehydrates, its characteristic H<sub>2</sub>O absorption bands at 1443 and 1945 nm shift to shorter wavelengths. Band depths and widths of absorptions at ~1200, 1400–1600, 1750, 1945, 2100–2200, and ~2400 nm all decrease with increasing temperature. The samples also underwent visible changes upon dehydration, both at the macroscopic and microscopic level, becoming very friable with an increase in fine grains. No consistent relationship was observed between dehydration temperature and grain size or habit. The samples were monitored for up to 20 months after dehydration, during which time none rehydrated to form gypsum. While the transition from gypsum to bassanite is very abrupt, bassanite does not readily rehydrate to form gypsum again in ambient conditions, and therefore may not be as unstable as previously thought by terrestrial occurrences of bassanite being predominantly restricted to hyperarid climates.

**Keywords:** Gypsum, bassanite, reflectance, spectroscopy, dehydration, sulfate, visible, near-infrared

### INTRODUCTION

Gypsum (CaSO<sub>4</sub>·2H<sub>2</sub>O) and bassanite (CaSO<sub>4</sub>·0.5H<sub>2</sub>O) are commonly formed on Earth in marine and saline lake evaporite sequences and hydrothermal systems. Other formation mechanisms of gypsum include hydration of primary anhydrite (CaSO<sub>4</sub>), as a reaction product of sulfuric acid and carbonate rocks in oxidizing sulfate deposits, and from sulfurous volcanic gases acting on Ca-bearing rocks. While gypsum is the most common terrestrial evaporite mineral, bassanite is much rarer, often forming via dehydration of primary gypsum. Bassanite can also form as a primary evaporite mineral in higher temperature settings, via desiccation of primary gypsum, or by evaporation of highly saline solutions (Peckmann et al. 2003; Vaniman and Chipera 2006). On Earth, bassanite is thought to only be stable in very arid climates, such as in certain soils in Egypt (Mees and De Dapper 2005), Australia (Arakel 1980), Death Valley (Hunt et al. 1966), and Kuwait (Gunatilaka et al. 1985). Often this stability is only seasonal, with the bassanite rehydrating to gypsum once wetter conditions return (e.g., Hunt et al. 1966; Gunatilaka et al. 1985). Gypsum has also recently been detected spectroscopically on Mars (e.g., Langevin et al. 2005; Wray et al. 2009), as well as bassanite (Wray et al. 2010), making these

minerals of interest to the Mars science community as they imply the former presence of water.

The primary goal of this study is to document the visible to near-infrared (VNIR) spectral behavior of the gypsum to bassanite transition and to investigate the stability of bassanite formed from dehydration of gypsum at ambient conditions. To do this, an experiment was conducted to dehydrate gypsum while observing how the absorption spectrum changed in the 350–2500 nm range upon dehydration. VNIR reflectance spectroscopy was chosen because it is widely used for both terrestrial and planetary remote sensing purposes and is often used to distinguish between hydrated mineral phases.

### GYPSON AND BASSANITE

Gypsum occurs in four main polycrystalline habits (e.g., Raman and Jayaraman 1954): alabaster, a white, semi-opaque aggregate of randomly oriented small crystals; massive, similar to alabaster but an aggregate of larger crystals; satin spar, a fibrous form with fibers lying along the crystallographic *c*-axis; selenite, a translucent aggregate of rods/sheets with their normal parallel to the *b*-axis. Bassanite occurs in two crystalline habits: large euhedral crystals and small, white acicular (needle-like) crystals (e.g., Hildyard et al. 2011).

The basic structural unit of gypsum is a chain of alternating edge-sharing SO<sub>4</sub> tetrahedra and CaO<sub>8</sub> polyhedra running parallel [101]. These chains are connected via shared edges of the CaO<sub>8</sub> to form corrugated layers parallel to {010} separated by layers

\* Present address: Malin Space Science Systems, P.O. Box 910148, San Diego, CA 92191, U.S.A. E-mail: harrison@msss.com

of H<sub>2</sub>O molecules. These H<sub>2</sub>O molecules bind the layers together with hydrogen bonds.

Bassanite is also made up of chains of edge-sharing SO<sub>4</sub> tetrahedra and CaO<sub>8</sub> polyhedra, but the chains are held together by the SO<sub>4</sub> ions rather than by H<sub>2</sub>O molecules. When bassanite absorbs water, the H<sub>2</sub>O molecules form hydrogen bonds with the SO<sub>4</sub> ions in the structure (Bezou et al. 1995; Chio et al. 2004).

The VNIR spectra of gypsum and bassanite were first detailed by Hunt et al. (1971), and later by Crowley (1991), Cloutis et al. (2006, 2008), and Clark et al. (2007), and are pictured in Figure 1. The ~1000 nm absorption band in gypsum was suggested by Crowley (1991) to be a combination of the first overtone of the O-H stretching and the first overtone of the H-O-H bending fundamentals. Crowley (1991) attributed the ~1200 nm absorption band in gypsum to be a combination of the H<sub>2</sub>O bending fundamental and the first overtone of the O-H stretching fundamental. The 1400–1600 nm triplet arises from O-H stretching (Cloutis et al. 2008). The 1940 and 1970 nm absorption bands in gypsum result from H<sub>2</sub>O combinations (Crowley 1991; Cloutis et al. 2008). The 1750 nm absorption was attributed to bending and stretching combinations of the H<sub>2</sub>O molecule by Crowley (1991) and Cloutis et al. (2006, 2008), while Hunt et al. (1971) states that this absorption may also be due to O-H bending and stretching or rotational fundamentals, or S-O bending overtones. Absorptions in the 2100–2200 nm range are due to S-O bending overtones (Cloutis et al. 2006) or OH/H<sub>2</sub>O combinations and/or overtones (Hunt et al. 1971; Cloutis et al. 2008), and a large absorption in the 2400 nm range arises from S-O stretching combinations (Cloutis et al. 2008).

The VNIR spectrum of bassanite exhibits all of the major H<sub>2</sub>O bands that are present in gypsum, but the bands are narrower and less structured (Hunt et al. 1971). Cloutis et al. (2008) describes the characteristic absorptions of bassanite. Two H<sub>2</sub>O combination and overtone bands occur in the 1400–1550 nm

range. While bassanite has only one H<sub>2</sub>O/O-H absorption feature in the 1700–1800 nm region, gypsum has two. The ~1940 nm H<sub>2</sub>O combination and overtone band in gypsum is also present in bassanite, but at a slightly shorter wavelength. An absorption of unknown origin near 2090 nm is present in bassanite, but not in gypsum. The S-O and/or H<sub>2</sub>O/O-H absorptions in the 2200 nm region in gypsum are not seen in bassanite.

## METHODS

### Gypsum dehydration experiment

Four gypsum samples constituting the main polycrystalline habits of gypsum (alabaster, massive, satin spar, and selenite) were obtained from Ward's Natural Science and dehydrated to examine changes in the reflectance spectrum over the 350–2500 nm wavelength region and to determine if habit has any effect on the behavior of a sample during dehydration. In one experiment, each sample was ground with an agate mortar in ethanol, sieved to two grain size fractions (<63 μm and 63–125 μm) and ultrasonicated to remove fine grains. Each sample was then heated in air in a gravity convection oven in 15 ± 5 °C increments for half an hour at each interval over the temperature range of 55–130 °C, with an additional step at 92 °C. This temperature range was chosen based on the wide range of temperatures given in the literature for the gypsum-bassanite transition (e.g., Bushuev et al. 1983; Chang et al. 1999; Prasad et al. 2001, 2005; Jordan and Astilleros 2006; Christensen et al. 2008; Ballirano and Melis 2009). At the end of each interval, the samples were removed from the oven, immediately weighed, and spectra were collected.

Each of the powdered samples was investigated at the beginning and the end of the experiment with a JEOL-6390LV scanning electron microscope (SEM) to examine grain morphology, as well as to verify the grain size of the samples after sieving. To verify what phase was formed in the dehydration experiments, each powdered sample was analyzed after the experimental runs via X-ray diffraction (XRD) using a hybrid Phillips/Norelco XRD with a copper tube and Dapple automation. The XRD patterns were normalized to quartz.

In a second experiment, hand samples (ranging from 28–140 g) of the four habits of gypsum were heated in 30 min increments from 55–115 °C and overnight at 130 °C to observe the differences between dehydration of powdered and hand samples of gypsum. The hand sample dehydration experiment was done to more realistically model gypsum dehydrating in an outcrop on a planetary surface.

### Laboratory spectroscopy

Spectra were collected with an ASD FieldSpec Pro FR spectroradiometer operating over the 350–2500 nm range. The spectroradiometer has a resolution of 3 nm at 700 nm, 10 nm at 1400 nm, and 12 nm at 2100 nm. A 512 element VNIR silicon photodiode array detector operates in the 350–1000 nm range, while two thermoelectrically cooled, graded index short-wave IR indium gallium arsenide photodiode detectors cover the 1000–2500 nm range. Each measurement was normalized to Spectralon to produce reflectance. Ten scans were collected and averaged for each sample at each temperature interval throughout the powdered and hand sample experiments. Spectral offsets in the data were present at 975 and 1781 nm where the second and third channels of the spectrometer began, and therefore the data were corrected to account for these offsets by shifting all of the data points in the first and third channels to match the reflectance level of the second channel. To better compare spectra, a continuum removal [a smoothed fitted curve to the spectrum representing background absorption (Aspinall et al. 2002)] was calculated for each spectrum using ENVI 4.3 (RSI Inc.). Spectral absorptions were quantified by measuring band depths (D<sub>b</sub>), defined by Clark and Roush (1984) as

$$D_b \equiv (R_c - R_b)/R_c \quad (1)$$

where R<sub>b</sub> is the reflectance at the band center and R<sub>c</sub> is the reflectance of the continuum at the band center.

## RESULTS

Spectra from the dehydration experiment using the powdered samples are pictured in Figures 2 and 3 (for a detailed listing of band positions vs. temperature for this experiment, see Harrison 2008). Significant spectral changes were observed in each sample with increasing temperature. The ~1200 nm absorption shifted to

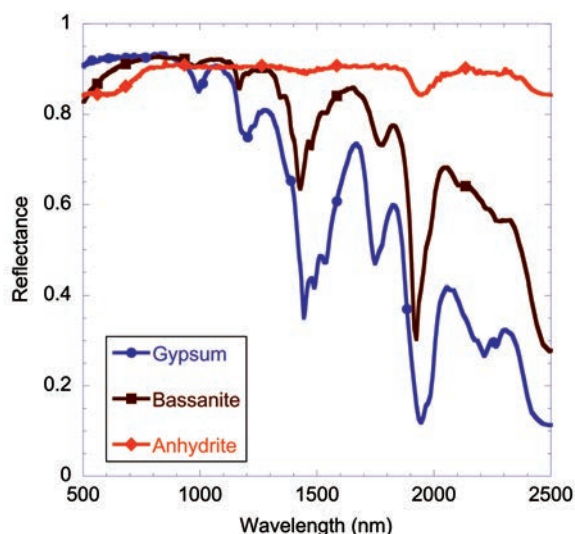


FIGURE 1. Spectra of gypsum (selenite from Washington Co., Utah), bassanite (gypsum heated at 60 °C), and anhydrite (gem show purchase, thought to be from New Mexico) from the USGS spectral library (Clark et al. 2007). (Color online.)

shorter wavelengths and became narrower upon dehydration. The 1750 nm absorption decreased in band depth, and disappeared altogether in some samples. Small absorptions at 2222 and 2227 nm decreased in band depth upon increasing temperature, with the shape of the spectrum in that region changing due to the gradual appearance of an absorption near 2100 nm and a decrease in depth of the large 2400 nm S-O absorption. The 1440 and 1940 nm H<sub>2</sub>O absorptions shifted to shorter wavelengths when the samples reached temperatures of ~92–115 °C (Fig. 4). Band depths and widths of these absorptions decreased with increasing temperature (Fig. 5). An absorption at ~1660 nm that

was not present in the original gypsum samples before grinding appeared at 55–70 °C and remained present throughout the experiment in some samples, whereas in others it appeared and disappeared at different temperature intervals. Upon dehydration, the third absorption in the 1400–1600 nm triplet began to disappear at 92–100 °C, with the triplet turning into a doublet. The shift in band positions at 100–115 °C results in a spectrum that matches the published spectrum of bassanite in the USGS spectral library, which was itself formed by the dehydration of gypsum at 60 °C for an unspecified amount of time (Crowley 1991). This ~100–115 °C temperature range also coincides

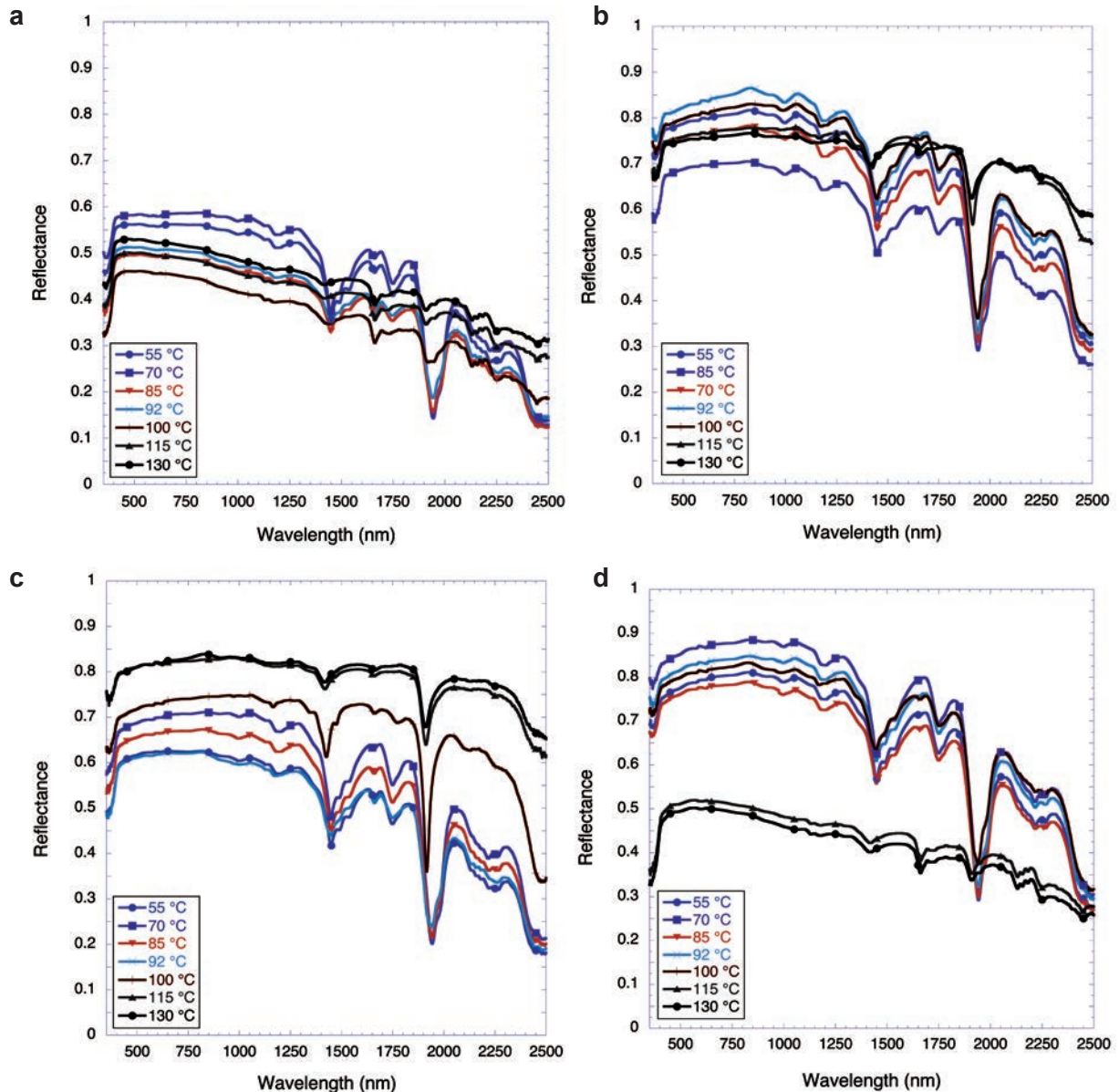


FIGURE 2. VNIR spectra of the <63 μm alabaster (a), massive (b), satin spar (c), and selenite (d) gypsum dehydration runs. Ten measurements were taken at each temperature interval and averaged together to produce these results. As the samples dehydrated, the band depths of the characteristic absorptions decreased and their wavelengths shifted; the 1200, 1440, and 1940 nm H<sub>2</sub>O bands shifted to shorter wavelengths while the 2400 nm S-O band shifted to longer wavelengths. The 1750 nm H<sub>2</sub>O and 2100–2200 nm S-O absorptions decrease in depth as the samples dehydrate, while an absorption forms around 2100 nm with increasing temperature. (Color online.)

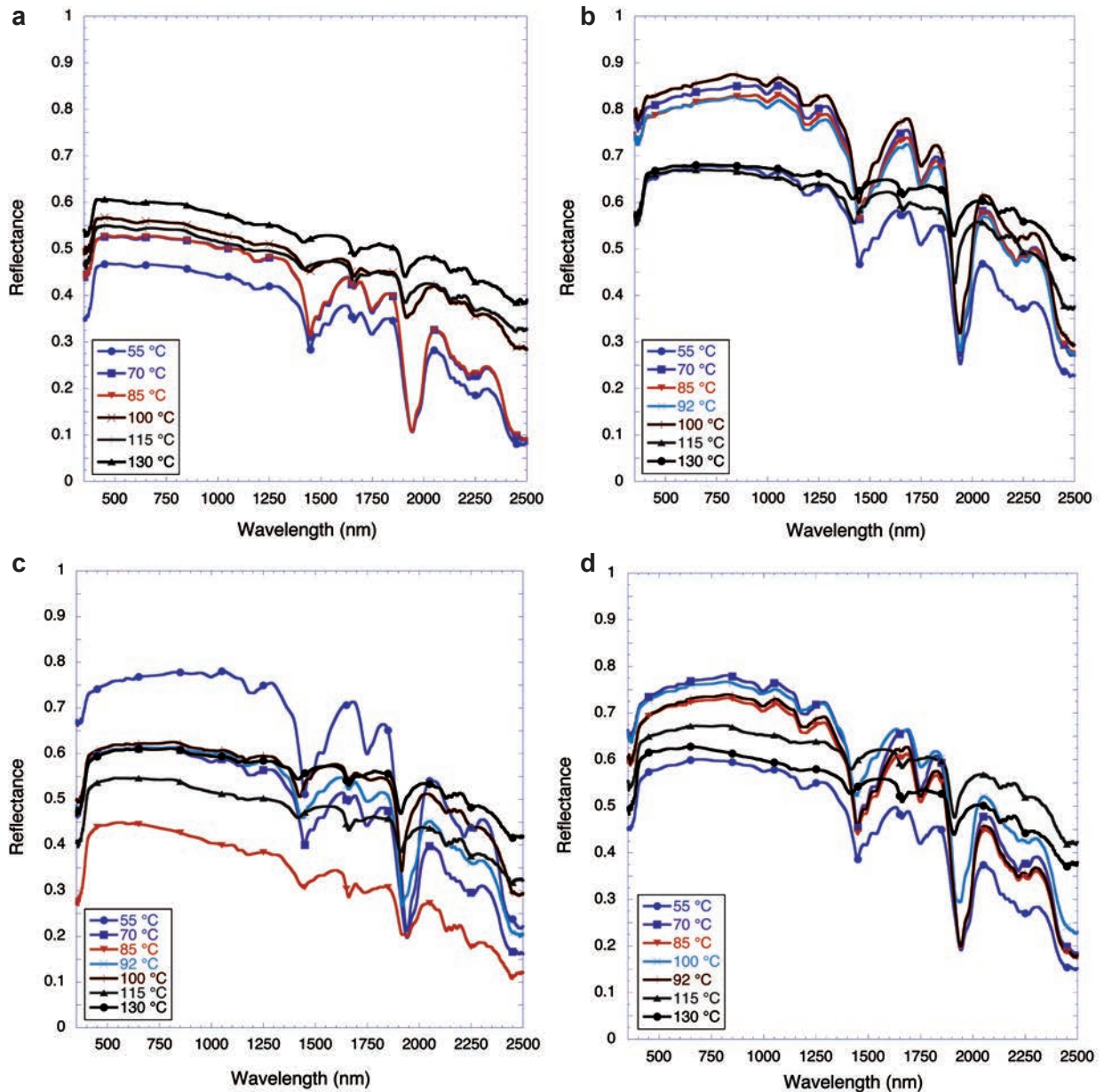


FIGURE 3. VNIR spectra of the 63–125  $\mu\text{m}$  alabaster (a), massive (b), satin spar (c), and selenite (d) powdered gypsum dehydration runs. See Figure 2 for experimental details. (Color online.)

with a peak in mass loss (interpreted as  $\text{H}_2\text{O}$  loss) (Fig. 6), with a peak at 100 °C for the <63  $\mu\text{m}$  samples and at 115 °C for the 63–125  $\mu\text{m}$  samples.

After the major shift in band positions observed at ~100–115 °C, the spectra of the samples continued to change with increasing temperature; band depths and widths of all of the aforementioned absorptions continued to decrease. The 1440 and 1940 nm bands shifted in total from ~1443 and ~1943 nm to ~1420 and ~1915 nm, respectively, over the entire 55–130 °C run. There is no consistent relationship between either grain size or habit and temperature at which the spectral changes occur in the 1440 and 1940 nm  $\text{H}_2\text{O}$  bands.

SEM observations show a greater number of fines in the samples after dehydration (Fig. 7). Some samples increased in reflectance from 100–130 °C, while others decreased in reflectance. The cause of this is unknown, as there are no obvious differences between the samples that increased in reflectance throughout the entire dehydration run and those whose reflectance eventually decreased.

Spectra of the hand sample dehydrations are shown in Figure 8. The spectra of the large gypsum crystals all shifted after being heated overnight at 130 °C except for the selenite sample, which changed to bassanite at 115 °C. Upon dehydration, the samples turned white and opaque and became very friable. An increase

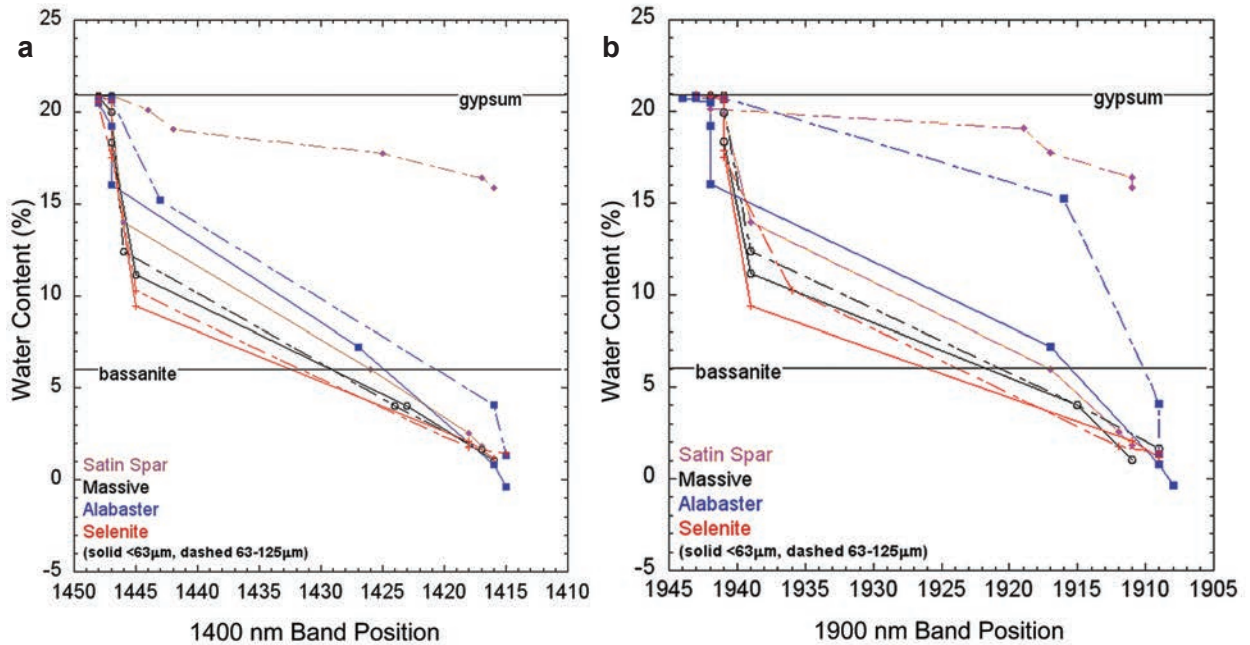


FIGURE 4. Band position vs. percentage of water lost for the 1440 nm (a) and 1900 nm (b) absorptions characteristic of gypsum. The 1400 and 1900 nm absorptions, caused by H<sub>2</sub>O combinations and overtones, shift to shorter wavelengths as water is lost (as temperature increases). (Color online.)

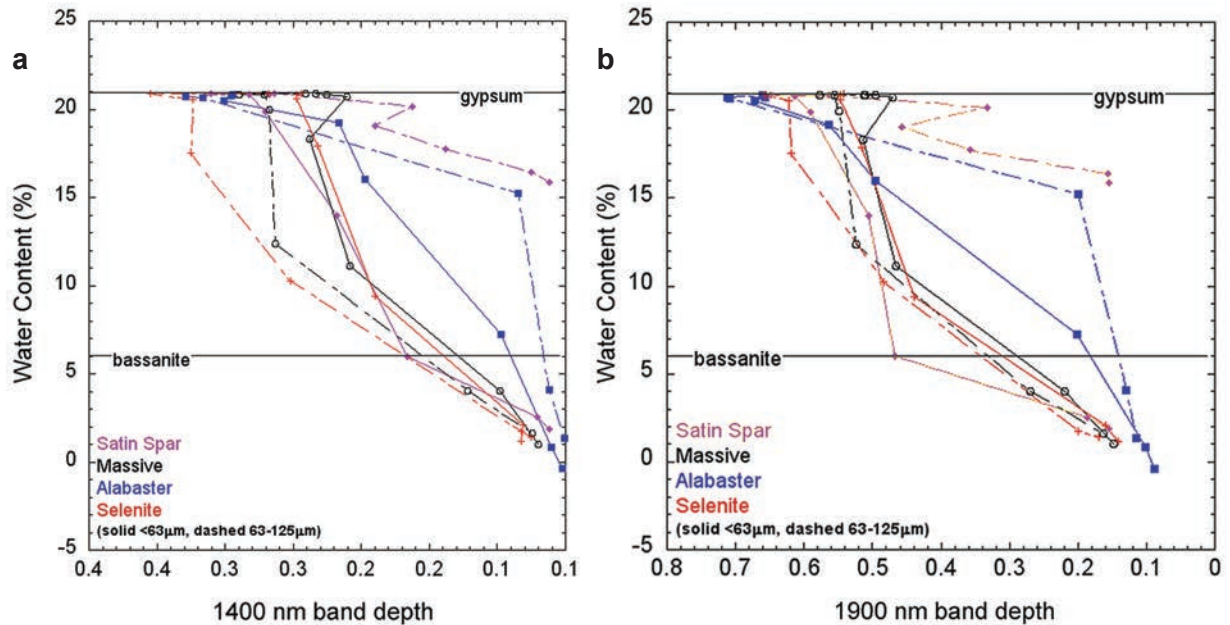
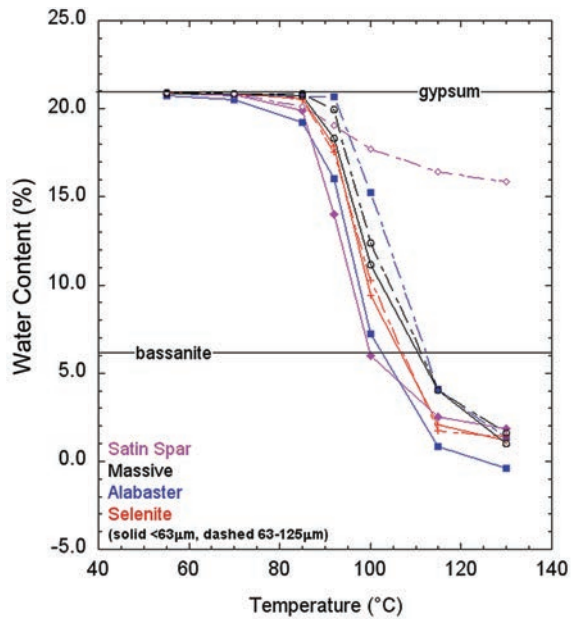


FIGURE 5. Absolute band depth vs. percentage of water lost for the 1440 nm (a) and 1940 nm (b) absorptions characteristic of gypsum. The band depth of both absorptions decreases as water is lost (as temperature increases). (Color online.)

in reflectance was observed in all of the hand-sample spectra between 100–130 °C. In all of the hand samples, the ~1448 and ~1943 nm bands shifted to 1420 and 1915 nm, respectively, upon dehydration, which are shorter wavelengths than those of bassanite (~1428 and 1925 nm).

After the dehydration experiments, the samples were stored in open Petri dishes on a lab bench with no control on temperature

and humidity (ambient humidity in the lab was ~20%), and their spectra were taken over a period of 20 months for the powdered samples (with the exception of the 63–125 μm satin spar sample, which was lost after 4 months) and 12 months for the hand samples (Figs. 9–11). In the dehydrated powdered samples, the bands at 1420 and 1915 nm shifted to 1428 and 1920 nm within one day of being removed from the oven at 130 °C, resulting in a spectrum



◀ **FIGURE 6.** Total mass (water) lost at each temperature interval for the dehydration of the powdered gypsum samples expressed as percentage of  $H_2O$  remaining in the sample. Gypsum contains 20.93% molecular weight  $H_2O$ , while bassanite contains 6.21%. Note the peaks at 100–115 °C, at the gypsum  $\rightarrow$  bassanite transition. (Color online.)

matching that of bassanite. The same band shift was observed in the dehydrated hand samples 4 h after being removed from the oven at 130 °C (the powdered samples were first measured one day after being removed from the 130 °C oven, whereas the hand samples were first measured at 4 h and then again at 28.5 h later). There were no further shifts in band position after this point in the 12–20 months the samples were observed. XRD patterns of each of the dehydrated samples were consistent with bassanite from the Caltech RRUFF database (Downs 2006).

### DISCUSSION

In all of the dehydration runs for the powdered samples, gypsum dehydrated at  $\sim 100$  °C, marked by a major shift in the positions of the hydration bands and a peak in water loss. This is consistent with Hunt et al. (1971) and the  $\sim 100$  °C that Sarma et

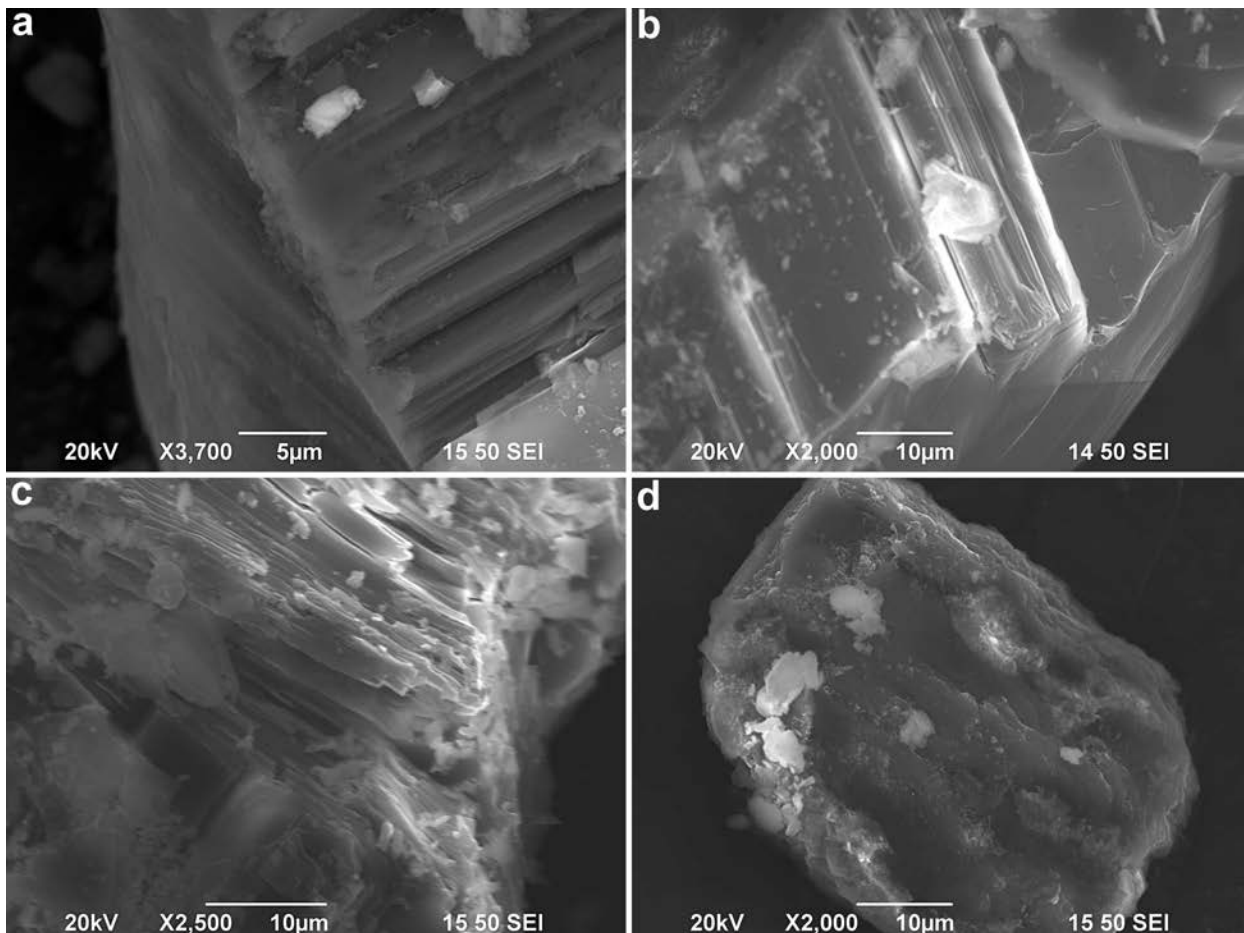


**FIGURE 7.** SEM images of powdered samples before and after dehydration. (a) Portion of a grain of 63–125  $\mu m$  massive gypsum before dehydration at 3700 $\times$  magnification. (b) Portion of a grain of  $<63$   $\mu m$  massive gypsum before dehydration at 2000 $\times$  magnification. (c) Portion of a grain of  $<63$   $\mu m$  satin spar gypsum after dehydration at 2500 $\times$  magnification. (d) Grain of  $<63$   $\mu m$  selenite after dehydration at 2000 $\times$  magnification. Note the smooth appearance of the gypsum in **a** and **b** compared to the heavily disrupted appearance of the bassanite in **c** and **d** due to the breakdown of the crystal structure.

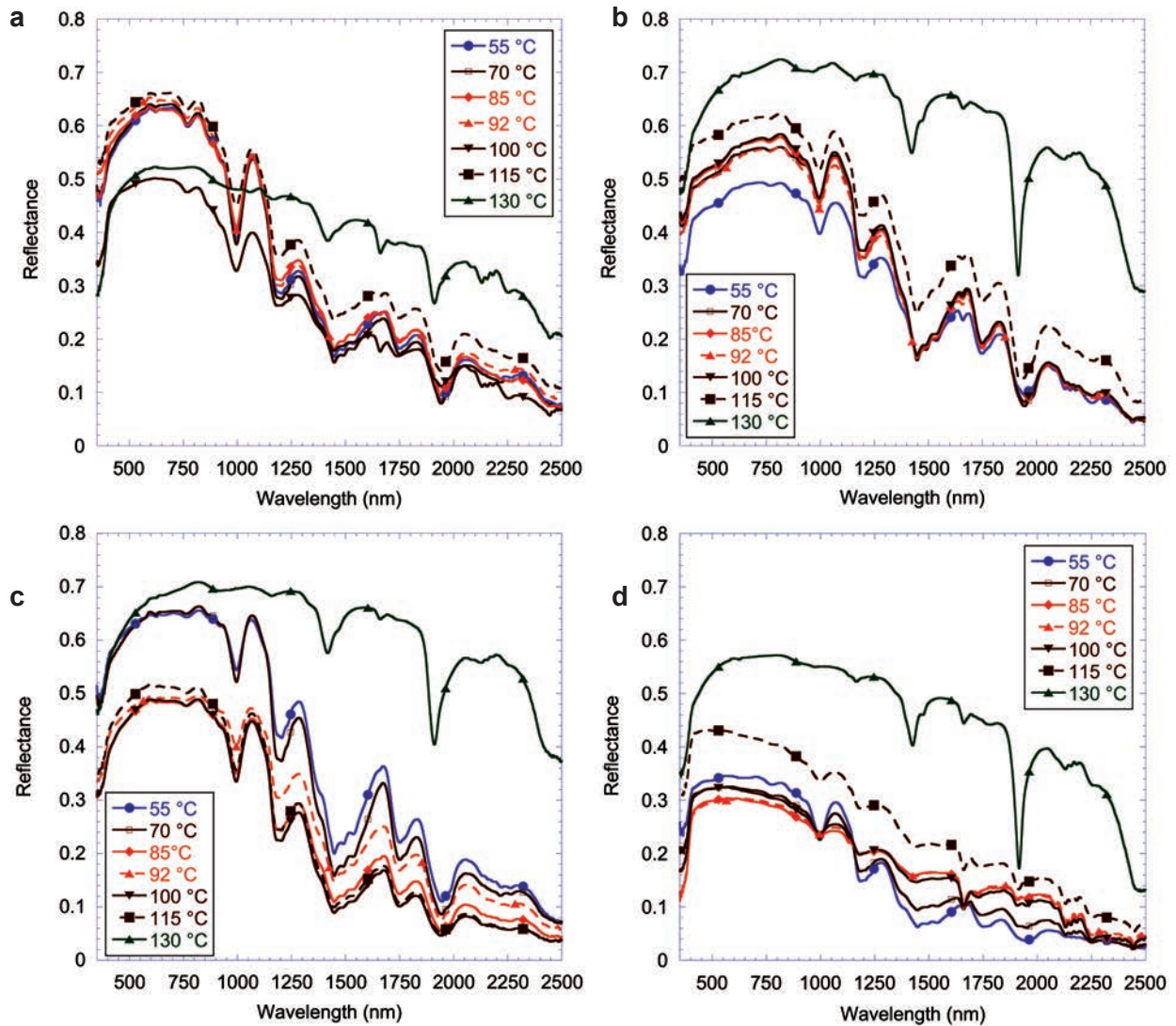


FIGURE 8. VNIR spectra of the dehydration of the gypsum hand samples. As the samples dehydrated, the band depths of the characteristic absorptions decreased and their wavelengths shifted; the 1200, 1440, and 1940 nm H<sub>2</sub>O bands shifted to shorter wavelengths while the 2400 nm S-O band shifted to longer wavelengths. The 1750 nm H<sub>2</sub>O and 2100–2200 nm S-O absorptions disappear as the samples dehydrate. (Color online.)

al. (1998) state is most generally accepted gypsum  $\rightarrow$  bassanite transition temperature. While this temperature is higher than the 85 °C found by Robertson and Bish (2007), in their experiment, dehydration of powdered gypsum did not start until the sample had been heated for 6.6 h. Therefore, the kinetics of the gypsum  $\rightarrow$  bassanite transition appears to accelerate with increasing temperature. Strydom et al. (1995) saw a “very small amount” of bassanite formation at 60 °C in experiments where synthetic gypsum was heated at an interval of 5 °C per minute, but state that the rate of dehydration was very slow at temperatures less than 95 °C. Experiments by Chang et al. (1999) did not observe bassanite formation until 118 °C at a relative humidity of 50%, indicating a dependence of the dehydration temperature on relative humidity as well.

The alabaster, massive, and satin spar hand samples of gypsum dehydrated at 130 °C while the selenite dehydrated at

115 °C. Sarma et al. (1998) and Prasad et al. (2001) both conducted dehydration experiments with small slabs of selenite, and found that bassanite formed at  $\sim$ 115 and  $\sim$ 96 °C, respectively. No other literature was found pertaining to the dehydration of hand samples of the other habits of gypsum. In the experiments detailed in this paper, the selenite was by far the smallest of the four hand samples ( $\sim$ 25 g while the other three were all over 100 g), which may have played a role in its lower dehydration temperature. The increase in reflectance from 100–130 °C is attributed to the increased number of fine-grained particles on the surface of the samples as the crystal structure was disrupted by the loss of H<sub>2</sub>O.

Previous experiments have shown that while powdered gypsum dehydrates first to bassanite and then to anhydrite, large crystals of gypsum dehydrate directly to CaSO<sub>4</sub> without an intermediate phase (Prasad et al. 2001, 2005; Sarma et al. 1998;

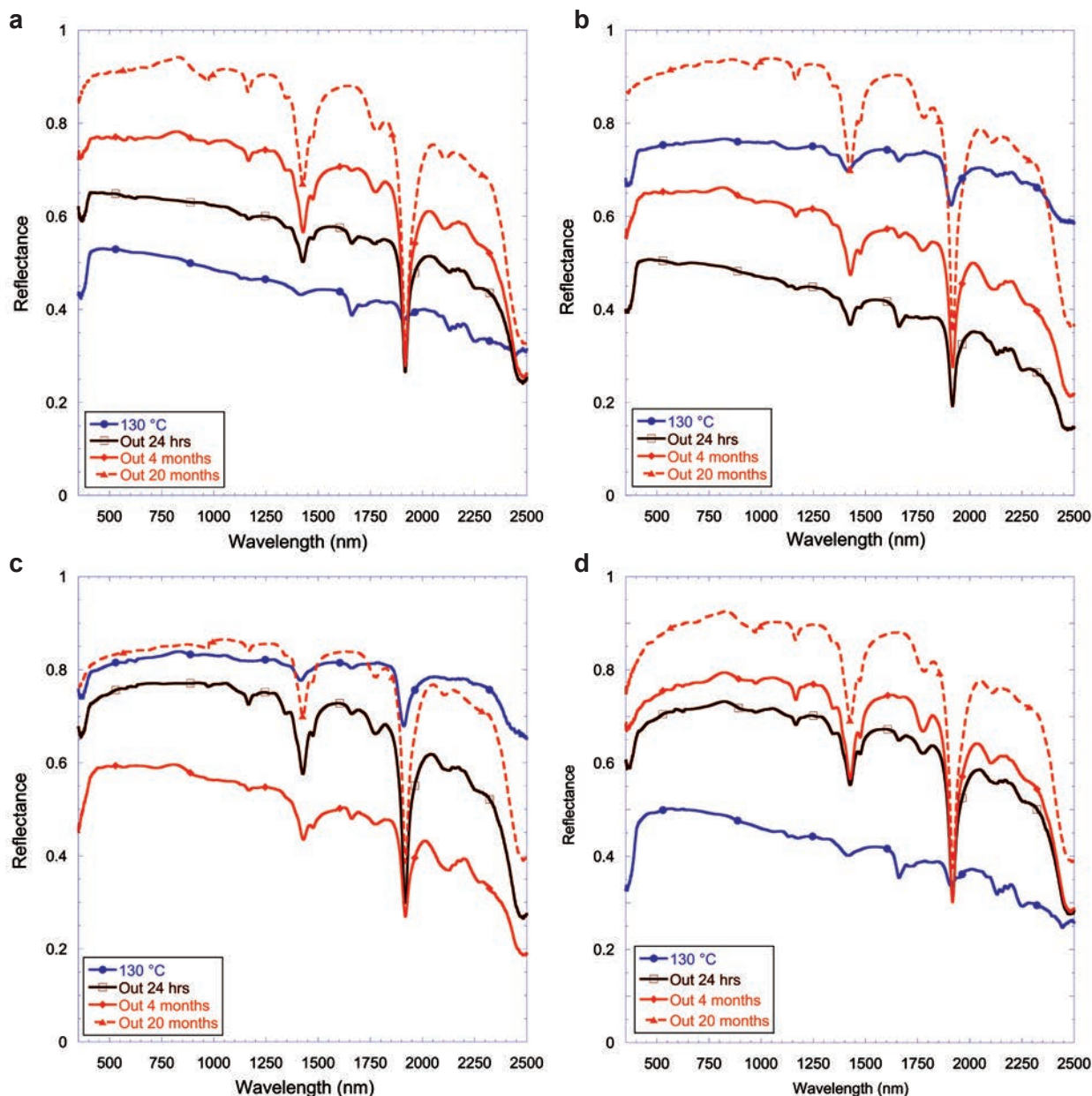


FIGURE 9. Spectra of the <math><63\ \mu\text{m}</math> alabaster (a), massive (b), satin spar (c), and selenite (d) gypsum samples at 130 °C, as well as 24 h, 4 months, and 20 months after being removed from the oven. The samples re-hydrated to bassanite within 24 h. While there were changes in the overall reflectance of the samples, the positions of the characteristic absorptions at 1440 and 1940 nm did not shift within the subsequent 20 months the samples were observed. The samples still had spectra consistent with bassanite after 20 months. (Color online.)

Putnis et al. 1990; Ballirano and Melis 2009). In the experiments described in this paper, the hand samples and powdered samples appeared to go from gypsum to bassanite and then to an intermediate phase between bassanite and anhydrite upon dehydration, but the spectrum of this intermediate phase is not consistent with either bassanite or soluble anhydrite because of the positions of the 1440 and 1940 nm absorptions, which are at shorter wavelengths than that of bassanite and are not present at all in anhydrite as these bands arise from  $\text{H}_2\text{O}$  molecules (i.e., Cloutis et al. 2006; Clark et al. 2007). This phase may be a

mixture of bassanite and anhydrite, or may be a calcium sulfate subhydrate ( $\text{CaSO}_4 \cdot n\text{H}_2\text{O}$ ,  $0 < n < 1.0$ ,  $n \neq 0.5$ ).

Cloutis et al. (2007) vacuum desiccated gypsum at 1 Pa and <math><25\ \text{°C}</math>. They observed a shift in the 1940 nm band to shorter wavelengths, an overall decrease in band depth, the 1440 nm triplet becoming “unrecognizable,” and the loss of the 1750 nm band. The results of the experiment detailed in this paper are consistent with the observations of Cloutis et al. (2007), who attribute these changes to structural rearrangement as the gypsum transitions to bassanite, with the  $\text{H}_2\text{O}$  bonds breaking and the  $\text{SO}_4$

bonds becoming stronger. The abrupt dehydration of gypsum to bassanite at 100–115 °C in my experiment is consistent with the kinetics described by Robertson and Bish (2007); in their experiments, no intermediate phases of calcium sulfate subhydrate were formed during the gypsum → bassanite transition. This lack of subhydrate formation has also been described by other experiments (Saito 1961; Ball 1977; Putnis et al. 1990; Chang et al. 1999; Ballirano and Melis 2009). However, dehydration experiments by others (Ramsdell and Partridge 1929; Frik and

Kuzel 1982; Bushuev and Borisov 1982; Abriel 1983; Kuzel 1987; Kuzel and Hauner 1987; Abriel et al. 1988; Bezou et al. 1995; Strydom et al. 1995; Vaniman et al. 2008) have reported the formation of subhydrate phases of  $\text{CaSO}_4 \cdot n\text{H}_2\text{O}$  with  $0.06 \leq n \leq 0.81$ . The fast ramping up of temperatures in my experiment may have prevented the formation of subhydrate phases between gypsum and bassanite. Bushuev et al. (1983) state that in ambient air or hydrothermal conditions of <300 °C, gypsum dehydration follows the path:

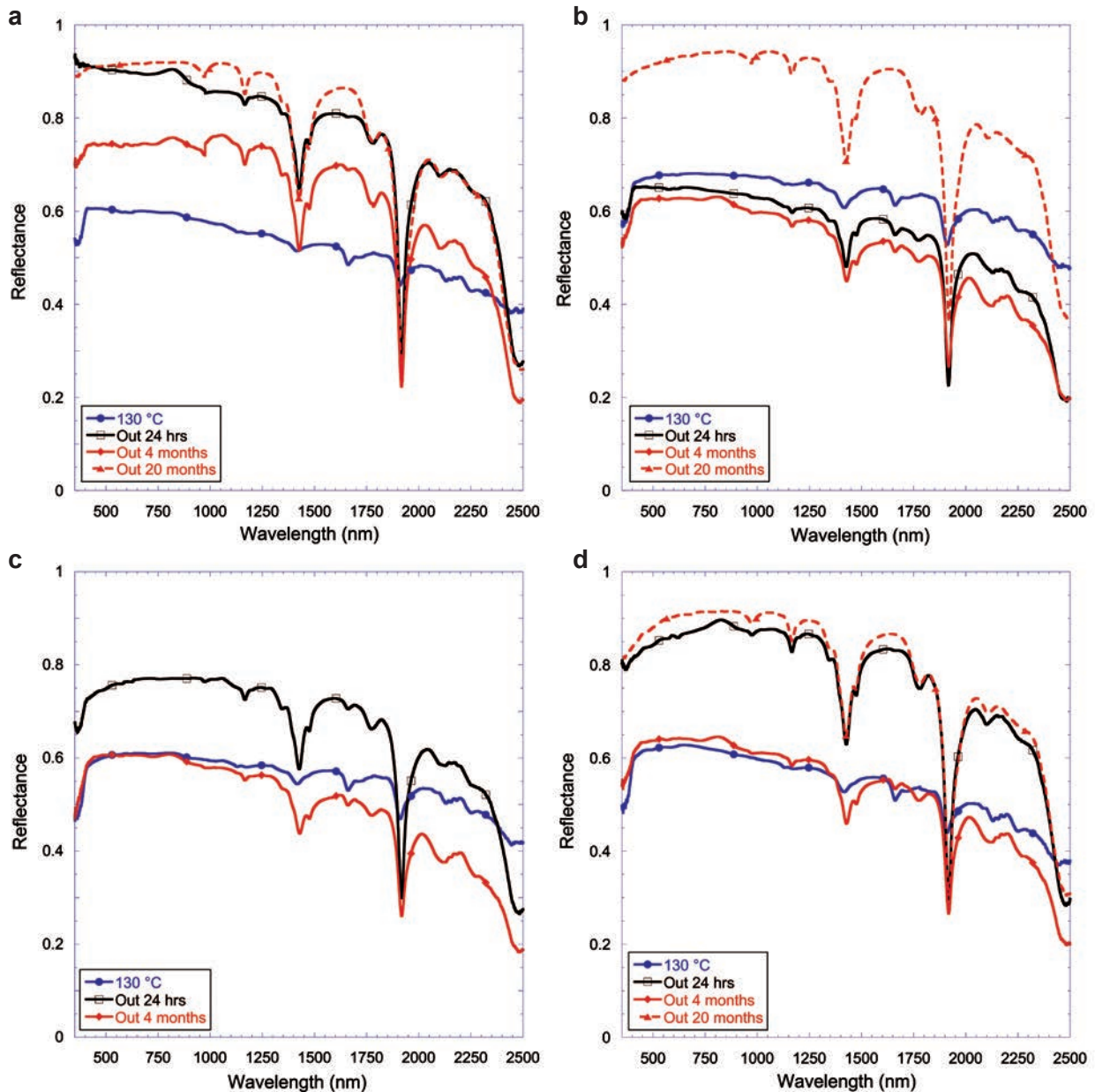


**FIGURE 10.** Spectra of the 63–125  $\mu\text{m}$  alabaster (a), massive (b), satin spar (c), and selenite (d) gypsum samples at 130 °C, as well as 24 h, 4 months, and 20 months (except for the satin spar 63–125  $\mu\text{m}$  sample, which was lost after 4 months) after being removed from the oven. The samples re-hydrated to bassanite within 24 h. While there were changes in the overall reflectance of the samples, the positions of the characteristic absorptions at 1440 and 1940 nm did not shift within the subsequent 20 months the samples were observed. The samples still had spectra consistent with bassanite after 20 months. (Color online.)

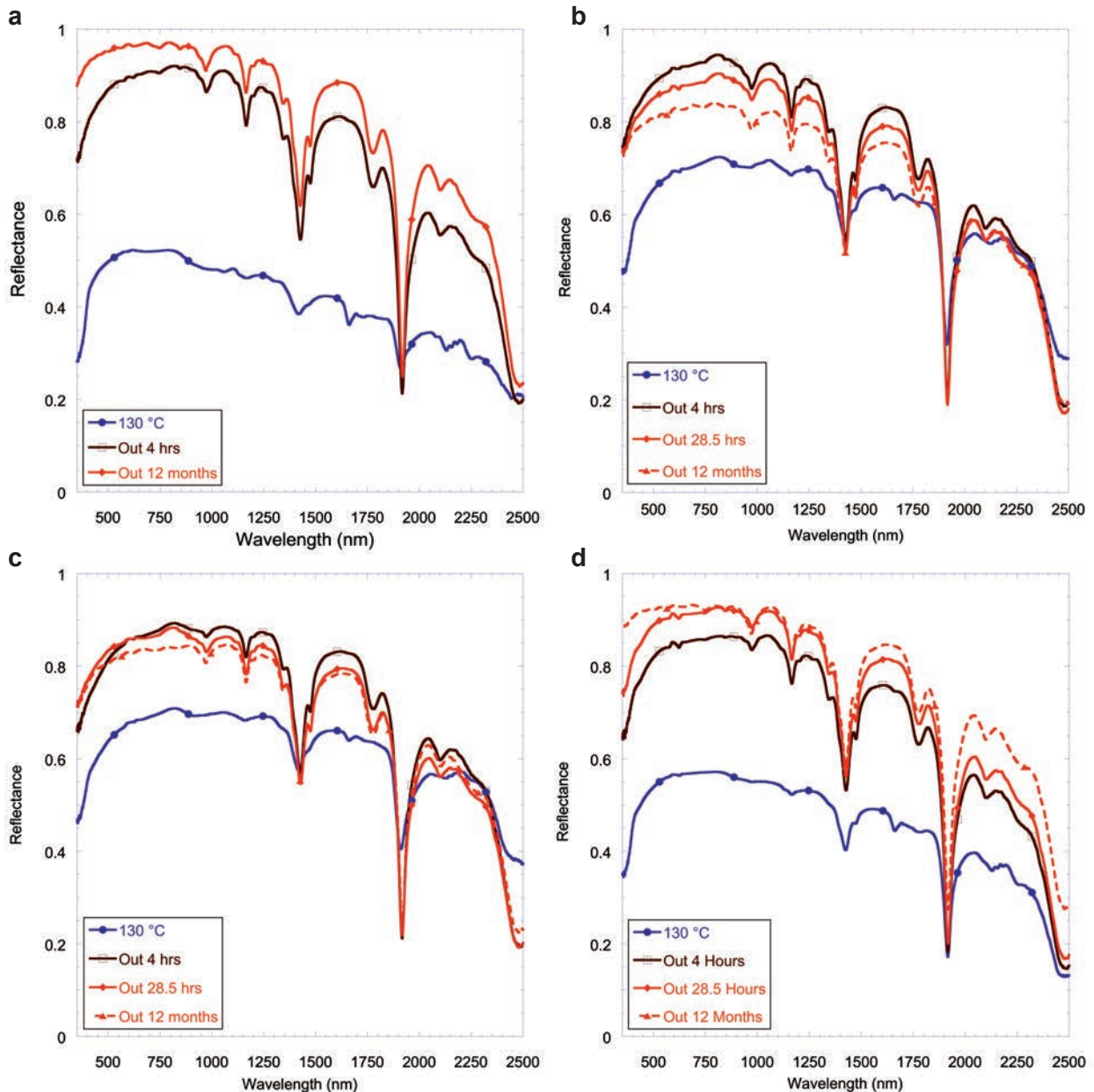
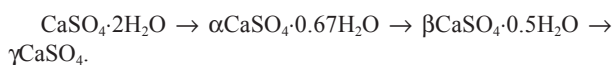


**FIGURE 11.** Spectra of the alabaster (a), massive (b), satin spar (c), and selenite (d) hand samples after 4 h and 12 months after being removed from the oven. The samples re-hydrated to bassanite within 4 h. While there were changes in the overall reflectance of the samples, the positions of the characteristic absorptions at 1440 and 1940 nm did not shift within the subsequent 12 months the samples were observed. The samples still had spectra consistent with bassanite after 12 months. (Color online.)



Ramsdell and Partridge (1929) conducted experiments in which gypsum was heated at temperatures of 120–180 °C for 17–120 h. Their samples lost on average 20.31% of their mass. Loss of 20.93% represents total dehydration, and therefore their experiments formed calcium sulfate subhydrate with  $n = 0.06$  (although they refer to it as “soluble anhydrite” in their paper).

This  $n = 0.06$  subhydrate was also formed via vacuum desiccation of gypsum by Vaniman et al. (2008), perhaps indicating that it is one of the unstable intermediate hydration states before total dehydration to anhydrite. The spectra of the powdered gypsum samples in my experiments continued to change after reaching bassanite, with the bands becoming shallower and shifting to shorter wavelengths, and therefore it appears that the samples either dehydrated past bassanite, forming a calcium sulfate subhydrate with  $n < 0.5$ . All of the samples except for the 63–125

$\mu\text{m}$  satin spar and  $<63 \mu\text{m}$  alabaster reached a phase containing between  $\sim 1\text{--}2\%$   $\text{H}_2\text{O}$  (Fig. 6) at  $130^\circ\text{C}$ .

After being removed from the oven, the depth of the 2100 nm absorption increased as the samples became more hydrated to form bassanite. This suggests that the 2100 nm absorption in bassanite arises from interaction between the absorbed  $\text{H}_2\text{O}$  molecules and the  $\text{SO}_4$  tetrahedra.

All of the samples had an increase in fines after dehydration. This is likely due to the gypsum structure breaking down as bassanite forms. Because  $\text{H}_2\text{O}$  molecules are essential to the crystal structure of gypsum, the structure is severely disrupted when it begins to dehydrate. This could result in pieces of grains breaking off as the crystal structure makes the shift from monoclinic (as in gypsum) to pseudo-hexagonal (as in bassanite), leading to an increase in fines in the sample. This should have resulted in an increase in reflectance in all of the samples, but some samples had a decrease in reflectance from  $100\text{--}130^\circ\text{C}$ . The cause of this is unknown, but may be due to differences in bulk habit or composition.

While the samples were left sitting out on a lab bench at ambient conditions, they rehydrated to form bassanite within the span of one day. Subsequent spectra taken repeatedly over the span of 12–20 months revealed that the samples remained bassanite and did not rehydrate to form gypsum, implying that the phase formed at  $130^\circ\text{C}$  was not stable in the ambient conditions of the lab and that bassanite is the favored stable phase as opposed to hydrating further to form gypsum. This is likely explained by the sample never being directly exposed to liquid water after dehydration. Bassanite in terrestrial settings has only been found to be stable in hyperarid environments, but in these locales the bassanite hydrates to form gypsum when exposed to water (e.g., rain or a rising water table). The results of my experiment suggest that bassanite will not rehydrate simply from adsorption of atmospheric water, and may therefore be stable indefinitely in ambient conditions as long as it is not exposed to liquid water.

#### ACKNOWLEDGMENTS

Thanks to Jim Gutmann of Wesleyan University for help in designing the dehydration experiment. Thanks are also due to Martha Gilmore for collecting the most recent bassanite spectra, and to James Greenwood and Joel Labela for help during experimental runs. This project was partially funded by the Connecticut Space Grant.

#### REFERENCES CITED

- Abriel, W. (1983) Calcium-sulfate subhydrate,  $\text{CaSO}_4 \cdot 0.8\text{H}_2\text{O}$ . *Acta Crystallographica*, 39, 956–958.
- Abriel, W., Reisdorf, K., and Pannetier, J. (1988) Kinetically-stable phases in gypsum dehydration. *Zeitschrift für Kristallographie*, 182, 270.
- Arakel, A.V. (1980) Genesis and diagenesis of Holocene evaporitic sediments in Hutt and Leeman lagoons, Western Australia. *Journal of Sedimentary Petrology*, 50, 1305–1326.
- Aspinall, R.J., Marcus, W.A., and Boardman, J.W. (2002) Considerations in collecting, processing, and analysing high spatial resolution hyperspectral data for environmental investigations. *Journal of Geographical Systems*, 4, 15–29.
- Ball, M.C. (1977) A discussion of the paper "The dehydration kinetics of calcium sulphate hydrate, influence of gaseous atmosphere and the temperature" by J.J. Gardet, B. Guilhot and M. Soustelle. *Cement and Concrete Research*, 7, 351–352.
- Ballirano, P. and Melis, E. (2009) Thermal behaviour and kinetics of dehydration of gypsum in air from in situ real-time laboratory parallel-beam X-ray powder diffraction. *Physics and Chemistry of Materials*, 36, 391–402.
- Bezou, C., Nonat, A., Mutin, J.C., Christensen, A.N., and Lehmann, M.S. (1995) Investigation of the crystal-structure of  $\gamma\text{CaSO}_4$ ,  $\text{CaSO}_4 \cdot 0.5\text{H}_2\text{O}$ , and  $\text{CaSO}_4 \cdot 0.6\text{H}_2\text{O}$  by powder diffraction methods. *Journal of Solid State Chemistry*, 117, 165–176.
- Bushuev, N.N. and Borisov, V.M. (1982) X-ray diffraction investigation of  $\text{CaSO}_4 \cdot 0.67\text{H}_2\text{O}$ . *Russian Journal of Inorganic Chemistry*, 27, 341–343.
- Bushuev, N.N., Maslennikov, B.M., and Borisov, V.M. (1983) Phase transformations in the dehydration of  $\text{CaSO}_4 \cdot 2\text{H}_2\text{O}$ . *Russian Journal of Inorganic Chemistry*, 28, 1404–1407.
- Chang, H., Huang, P.J., and Hou, S. (1999) Application of thermo-Raman spectroscopy to study the dehydration of  $\text{CaSO}_4 \cdot 2\text{H}_2\text{O}$  and  $\text{CaSO}_4 \cdot 1/2\text{H}_2\text{O}$ . *Materials Chemistry and Physics*, 58, 12–19.
- Chio, C.H., Sharma, S.K., and Munenow, D.W. (2004) Micro-Raman studies of gypsum in the temperature range between 9 K and 373 K. *American Mineralogist*, 89, 390–395.
- Christensen, A.N., Olesen, M., Cerenius, Y., and Jensen, T.R. (2008) Formation and transformation of five different phases in the  $\text{CaSO}_4 \cdot \text{H}_2\text{O}$  System: Crystal structure of the subhydrate  $\beta\text{-CaSO}_4 \cdot 0.5\text{H}_2\text{O}$  and soluble anhydrite  $\text{CaSO}_4$ . *Chemistry of Materials*, 20, 2124–2132.
- Clark, R.N. and Roush, T.L. (1984) Reflectance spectroscopy: Quantitative analysis techniques for remote sensing applications. *Journal of Geophysical Research*, 89, 6329–6340.
- Clark, R.N., Swayze, G.A., Wise, R., Livo, E., Hoefen, T., Kokaly, R., and Sutley, S.J. (2007) USGS digital spectral library splib06a: U.S. Geological Survey, Digital Data Series 231.
- Cloutis, E.A., Hawthorne, F.C., Mertzman, S.A., Krenn, K., Craig, M.A., Marcino, D., Methot, M., Strong, J., Mustard, J.F., Blaney, D.L., Bell, J.F., and Vilas, F. (2006) Detection and discrimination of sulfate minerals using reflectance spectroscopy. *Icarus*, 184, 121–157.
- Cloutis, E.A., Craig, M.A., Mustard, J.M., Kruzelecky, R.V., Jamroz, W.R., Scott, A., Bish, D.L., Poulet, F., and Bibring, J.-P. (2007) Stability of hydrated minerals on Mars. *Geophysical Research Letters*, 34, L20202.
- Cloutis, E.A., Craig, M.A., Kruzelecky, R.V., Jamroz, W.R., Scott, A., Hawthorne, F.C., and Mertzman, S.A. (2008) Spectral reflectance properties of minerals exposed to simulated Mars surface conditions. *Icarus*, 195, 140–168.
- Crowley, J.K. (1991) Visible and Near-Infrared (0.4–2.5 $\mu\text{m}$ ) Reflectance spectra of playa evaporite minerals. *Journal of Geophysical Research*, 96, 16231–16240.
- Downs, R.T. (2006) The RRUFF Project: an integrated study of the chemistry, crystallography, Raman and infrared spectroscopy of minerals. Program and Abstracts of the 19th General Meeting of the International Mineralogical Association, Kobe, Japan, no. O03-13.
- Frik, M. and Kuzel, H.-J. (1982) Röntgenographische und thermoanalytische Untersuchungen an Calciumsulfat-Halbhydrat. *Fortschritte der Mineralogie*, 60, 80–81.
- Gunatillaka, A., All-Temeemi, A., Saleh, A., and Nassar, N. (1985) A new occurrence of bassanite in recent evaporitic environments, Kuwait, Arabian Gulf. *University of Kuwait Journal (Science)*, 12, 157–166.
- Harrison, T.N. (2008) Origin and composition of the light-toned layered deposits in Iani Chaos, Mars, 147 p. M.A. thesis, Wesleyan University, Middletown, Connecticut.
- Hildyard, R.C., Llana-Fúnez, S., Wheeler, J., Faulkner, D.R., and Prior, D.J. (2011) Electron backscatter diffraction (EBSD) analysis of bassanite transformation textures and crystal structure produced from experimentally deformed and dehydrated gypsum. *Journal of Petrology*, 52, 839–856.
- Hunt, C.B., Robinson, T.W., Bowles, W.A., and Washburn, A.L. (1966) Hydrologic basin Death Valley, California. U.S. Geological Survey Paper 494-B, 1–138.
- Hunt, G.R., Salisbury, J.W., and Lenhoff, C.J. (1971) Visible and near-infrared spectra of minerals and rocks. VI. Sulfides and sulfates. *Modern Geology*, 3, 1–14.
- Jordan, G. and Astilleros, J.M. (2006) In-situ HFAM study of the thermal dehydration of gypsum (010) surfaces. *American Mineralogist*, 91, 619–627.
- Kuzel, H.-J. (1987) Hydratationswärmen von  $\alpha$ -Calcium-sulfaten. *Neues Jahrbuch für Mineralogie*, 156, 155–174.
- Kuzel, H.-J. and Hauner, M. (1987) Chemische und kristallographische Eigenschaften von Calciumsulfate-Halbhydrat und Anhydrit III. *Zement Kalk Gips*, 40, 628–632.
- Langevin, Y., Poulet, F., Bibring, J.-P., and Gondet, B. (2005) Sulfates in the north polar region of Mars detected by OMEGA/Mars Express. *Science*, 307, 1584–1586.
- Mees, F. and De Dapper, M. (2005) Vertical variations in bassanite distribution patterns in near-surface sediments, southern Egypt. *Sedimentary Geology*, 181, 225–229.
- Peckmann, J., Goedert, J.L., Heinrichs, T., Hoefs, J., and Reitner, J. (2003) The Late Eocene "Whiskey Creek" methane-seep deposit (Western Washington State)—Part II: Petrology, stable isotopes, and biogeochemistry. *Facies*, 48, 241–253.
- Putnis, A., Winkler, B., and Fernandez-Diaz, L. (1990) In situ IR spectroscopic and thermogravimetric study of the dehydration of gypsum. *Mineralogical Magazine*, 54, 123–128.
- Prasad, P.S.R., Pradhan, A., and Gowd, T.N. (2001) In-situ micro-Raman investigation of dehydration mechanism in natural gypsum. *Current Science*, 80, 1203–1207.
- Prasad, P.S.R., Chaitanya, V.K., Prasad, K.S., and Rao, D.N. (2005) Direct formation

- of the  $\gamma$ -CaSO<sub>4</sub> phase in dehydration process of gypsum: In situ FTIR study. *American Mineralogist*, 90, 672–678.
- Raman, C.V. and Jayaraman, A. (1954) X-ray studies on polycrystalline gypsum. *Proceedings of the Indian Academy of the Sciences, A*, 40, 57–60.
- Ramsdell, L.S. and Partridge, E.P. (1929) The crystal forms of calcium sulphate. *American Mineralogist*, 14, 59–74.
- Robertson, K. and Bish, D. (2007) The dehydration kinetics of gypsum: The effect of relative humidity on its stability and implications in the martian environment. *Lunar and Planetary Science XXXVIII*, Houston, no. 1432.
- Saito, T. (1961) Some observations on the process of dehydration and rehydration of gypsum by means of proton magnetic resonance. *Bulletin of the Chemical Society of Japan*, 34, 1454–1457.
- Sarma, L.P., Prasad, P.S.R., and Ravikumar, N. (1998) Raman spectroscopic study of phase transitions in natural gypsum. *Journal of Raman Spectroscopy*, 29, 851–856.
- Strydom, C.A., Hudson-Lamb, D.L., Potgieter, J.H., and Dagg, E. (1995) The thermal dehydration of synthetic gypsum. *Thermochimica Acta*, 269/270, 631–638.
- Vaniman, D.T. and Chipera, S.J. (2006) Transformations of Mg- and Ca-sulfate hydrates in Mars regolith. *American Mineralogist*, 91, 1628–1642.
- Vaniman, D.T., Bish, D.L., and Chipera, S.J. (2008) Calcium Sulfate Hydration, Stability and Transformation on Mars. *Lunar and Planetary Science XXXIX*, Houston, no. 1391.
- Wray, J.J., Murchie, S.L., Squyres, S.W., Seelos, F.P., and Tornabene, L.L. (2009) Diverse aqueous environments on ancient Mars revealed in the southern highlands. *Geology*, 37, 1043–1046.
- Wray, J.J., Squyres, S.W., Roach, L.H., Bishop, J.L., Mustard, J.F., Dobre, E.Z.N. (2010) Identification of the Ca-sulfate bassanite in Mawrth Vallis, Mars. *Icarus*, 209, 416–421.

MANUSCRIPT RECEIVED AUGUST 2, 2010  
MANUSCRIPT ACCEPTED DECEMBER 14, 2011  
MANUSCRIPT HANDLED BY M. DARBY DYAR